

Effects of Metal Ion Binding on an Oncomodulin Mutant Containing a Novel Calcium-Binding Loop

Ian D. Clark,¹ Andromeda J. Bruckman,¹ Christopher W. V. Hogue,² John P. MacManus,¹ and Arthur G. Szabo^{3,4}

Received November 28, 1993; revised June 13, 1994; accepted June 14, 1994

The Ca²⁺-binding protein oncomodulin was altered by cassette mutagenesis of the CD site (CDOM33) with a sequence that was derived by a consensus method using over 250 known Ca²⁺-binding loop sequences. This mutant was studied using time-resolved and steady-state fluorescence from the Trp residue included at position 7 of the loop (position 57 of the protein sequence). The fluorescence characteristics of this species in the absence and presence of metal ions were compared to those of a tetradecapeptide containing the loop and the single Trp mutant of oncomodulin, Y57W. The fluorescence properties of CDOM33 were quite different from the peptide, both in the apo form and in response to metal binding. The consensus CD loop in CDOM33 exhibited the characteristics of a Ca²⁺/Mg²⁺ site in contrast to the Ca²⁺ specificity of the wild-type CD loop. The Trp analogue, 5-hydroxytryptophan (5HW), was incorporated into both oncomodulin mutants to produce Y75(5HW) and 5HW-CDOM33. Results showed that this intrinsic probe was relatively insensitive to structural changes in the mutants upon metal binding compared to Trp itself.

KEY WORDS: Oncomodulin; tryptophan; 5-hydroxytryptophan; fluorescence; calcium binding; terbium.

INTRODUCTION

Calcium-binding proteins have evolved to perform a wide range of functions, many of which are regulated by the binding of the metal ion. A subgroup of this family consists of proteins with the structural motif, α -helix-loop- α -helix (HLH or "EF hand"), that bind calcium in the loop portion. In these proteins, the HLH motif occurs pairwise, with each loop portion consisting of 12 contiguous residues which provide oxygen ligands for the calcium ion. These loops are further designated within an individual protein by the numbering of the helices between which they are found. Thus the CD loop or EF loop is the loop lying between the C and the D helices

or the E and the F helices, respectively. The side chains of the loop residues 1, 3, 5, 9, and 12 are involved in chelation of Ca²⁺ along with the backbone carbonyl of residue 7. In addition, some hydrogen bonding occurs between adjacent loop motifs, forming an antiparallel β -sheet which contributes to structural stability [1].

Examination of the sequences of >250 Ca²⁺-binding loop sequences [2] showed considerable homology, within the 12-residue sequence—notably with Asp(1), Asp(3), Gly(6), and Glu(12). MacManus *et al.* [3] prepared loop peptides with a consensus sequence derived from the known sequences, modifying Asp(3) to Asn(3) to minimize charge repulsion. Their motivation for the design and eventual incorporation of this consensus sequence into oncomodulin was to engineer this protein so that the metal-binding affinity of one of its two metal-binding loops was significantly greater than the native group. This was aimed at determining structural parameters which controlled the metal-binding affinity. A Trp residue was incorporated into position 7 of the loop (position 57 in the protein) so that efficient energy trans-

¹ Institute for Biological Sciences, National Research Council, Ottawa, Ontario, Canada.

² Department of Biochemistry, University of Ottawa, Ottawa, Ontario, Canada.

³ Department of Chemistry and Biochemistry, University of Windsor, Windsor, Ontario, Canada N9B 3P4.

⁴ To whom correspondence should be addressed.

fer to a bound luminescent terbium ion would be achieved. The earlier peptide work had shown that Trp located in such a position was the most effective for this purpose. The sequence that was subsequently included into the rat oncomodulin CD loop site by cassette mutagenesis was DKNADGWIEFEE [4]. The Trp residue is at position 57 of the mutant protein sequence (Tyr57 in native oncomodulin). The product was named CDOM33 as a shorthand form of CD loop of oncomodulin (OM) replaced by peptide 33 [3]. This is different from the wild-type CD loop sequence, DNDQSGYLDGDE, at every position except 1, 6, and 12. Using the fluorescence of the single Trp mutant in the CD loop of the wild-type protein, Y57W [5], it was shown that Ca^{2+} binding caused significant structural change in the loop region. In Y57W, the EF site has the higher affinity, filling first upon Ca^{2+} addition [6,7], and this is responsible for 80% of the total fluorescence change from Trp-57 in the CD loop. In the cassette mutant, the order of fill of the two sites was reversed—CD then EF—as determined by Tb^{3+} titration [4], reflecting the increased metal affinity of the consensus sequence relative to the wild-type sequence in the CD loop. The side-chain carboxylate group of Asp at position 9 of the native CD loop chelates to Ca^{2+} via at least one bridging water molecule, whereas with Glu-9 of the consensus sequence the carboxylate group chelates directly. This effect is consistent with the observations of Falke *et al.* [8], who showed that the trivalent ion binding affinity increases significantly with the number of negatively charged chelating side chains.

Recently 5-hydroxytryptophan (5HW) was incorporated into oncomodulin at position 57 to produce the mutant Y57(5HW) [9]. This new intrinsic probe has fluorescence properties similar to those of Trp but has an extended absorption spectrum to lower energy, allowing selective excitation in the presence of Trp residues in other proteins and hence allowing investigation of protein–protein interactions.

In this study, the structural changes in the oncomodulin CD loop cassette mutant (CDOM33) upon metal binding are compared to those in a 14mer cassette peptide (Pep 33) and the Y57W mutant, using both Trp and 5-OH Trp fluorescence.

MATERIALS AND METHODS

Peptide and protein samples were prepared as reported previously [3–5,9–11]. All proteins, with the exception of 5HW-CDOM33, were dissolved in 100 mM KCl, 10 mM Pipes, pH 6.5, and made apo by trichlo-

roacetic acid (TCA) precipitation [5]. Due to the very small quantity of 5HW-CDOM33 available, apo protein was made by the addition of 1 mM EGTA to the buffer. Typically, fluorescence lifetimes were measured on 5 μM protein in the absence or presence of 20 μM Ca^{2+} , 20 μM Tb^{3+} , or 1 mM Mg^{2+} .

Fluorescence lifetimes were measured on a time-correlated single-photon counting instrument [12]. The excitation source was a cavity-dumped dye laser synchronously pumped by an actively mode-locked argon ion laser (Spectra Physics), operating at 825 kHz with a pulse width of 15 ps. The instrument was constructed in a T-format configuration, with each detection line containing a polarizer set at 55° to the vertical, a JY H10 monochromator (4-nm band pass), and a Hamamatsu 1564U-01 microchannel plate photomultiplier. The channel width was 10 ps and data were collected in 2048 channels of a multichannel analyzer. The instrument response function at the 295-nm excitation wavelength was determined from the Raman scattering of H_2O at 326 nm [13]. For 310-nm excitation of 5HW-containing samples, Raman scattering was measured at 346 nm. Each sample decay curve typically contained 2×10^6 total counts and required 5 min for data collection. A “no-protein” blank was measured for each sample for the same accumulation time and the blank counts subsequently subtracted from the sample decay curve. Data were analyzed by a nonlinear least-squares iterative convolution method based on the Marquardt algorithm [14]. The fits to sums of exponentials were deemed adequate when the reduced χ^2 parameter (Bevington, 1969) was less than 1.10 and/or the serial variance ratio (SVR) [15] was between 1.80 and 2.10 [16]. Fluorescence decay data at different emission wavelengths confirmed that τ_i (decay time of the *i*th component) was independent of wavelength. This allowed a global analysis of the data measured across the fluorescence spectrum [17].

Decay-associated spectra (DAS), the emission spectra associated with each individual decay component [18], were calculated from

$$I_i(\lambda) = I_{ss}(\lambda) [\alpha_i(\lambda)\tau_i/\sum\alpha_i(\lambda)\tau_i] \quad (1)$$

where $I_i(\lambda)$ is the emission intensity associated with the *i*th component, $I_{ss}(\lambda)$ is the total steady-state intensity, and $[\alpha_i(\lambda)\tau_i/\sum\alpha_i(\lambda)\tau_i]$ is the fractional fluorescence of the *i*th component, measured at wavelength λ . The fractional concentration of each component was calculated by dividing the area of each DAS_{*i*} by the lifetime, τ_i , and scaled to sum to 1.00.

Steady-state fluorescence measurements (corrected) were made on a SLM 8000C spectrofluorimeter, 4-nm

Table I. Time-Resolved Fluorescence Parameters of Tryptophan in Peptide 33 and CDOM Protein^a

	τ_1 (ns)	τ_2 (ns)	τ_3 (ns)	C_1	C_2	C_3	χ^2	SVR
Peptide 33								
Apo	3.73	1.58	0.23	0.31	0.47	0.22	1.1	1.78
Ca ²⁺ loaded	3.71	1.55	0.21	0.32	0.47	0.21	1.09	1.78
Mg ²⁺ loaded	3.56	1.55	0.27	0.36	0.46	0.18	1.07	1.82
Tb ³⁺ loaded	3.48	1.42	0.24	0.28	0.50	0.22	1.06	1.84
CDOM33								
Apo	5.81	1.64	0.27	0.29	0.57	0.14	1.03	1.94
Ca ²⁺ loaded	5.15	1.48	0.22	0.34	0.50	0.16	1.06	1.86
Mg ²⁺ loaded	4.55	1.83	0.31	0.26	0.54	0.20	1.06	1.89
Tb ³⁺ loaded	1.66	0.56	0.15	0.04	0.74	0.22	1.09	1.86
5HW-CDOM33								
Apo	3.31	1.00		0.82	0.18		1.09	1.70
Ca ²⁺ loaded	3.36	1.04		0.81	0.19		1.04	1.97
Mg ²⁺ loaded	3.35	1.27		0.62	0.38		1.09	1.77
Tb ³⁺ loaded	1.49	0.46		0.58	0.42		1.09	1.75

^a $C_1 + C_2 + C_3 = 1$, where $C_i = (\text{DAS}_i \text{ area}/\tau_i)$. DAS, decay-associated spectrum. Typical SE: $\tau_1 = \pm 0.01$ ns; $\tau_2 = \pm 0.02$ ns; $\tau_3 = \pm 0.002$ ns. Error in C_i no more than 5%.

slits at 20°C, with all sample absorbances less than 0.1 at the excitation wavelength to avoid any inner filter effect. Ca²⁺ and Mg²⁺ titrations were carried out on 5 μM apo samples in 1 \times 1-cm cells containing a stirring bar. Small aliquots of Ca²⁺ or Mg²⁺ stock solutions were added and fluorescence intensities were obtained, using 290-nm excitation and 350-nm emission [5]. Absorption spectra were measured on a Varian DMS 200 spectrophotometer, with quantum yields calculated using $\phi_f = 0.14$ for *N*-acetyltryptophanamide (NATA) at 20°C. This value was recently redetermined in our laboratory using 2-aminopyridine as a primary standard, having $\phi_f = 0.65$ in 1 *N* H₂SO₄ [19].

RESULTS

Table I shows the fluorescence parameters of CDOM33, 5HW-CDOM33, and peptide 33 (*GDKNADGWIEFEEL*) [3] in the apo, Ca²⁺-loaded, Mg²⁺-loaded, and Tb³⁺-loaded forms. It can be seen that the cassette mutagenesis of oncomodulin to CDOM33, by replacement of the CD loop with the loop portion of peptide 33 (residues 1–13 of the peptide), altered the structure of the peptide in the region around the Trp residue. This is manifested in significant differences in the lifetimes and relative concentrations (from integrated DAS) of the Trp fluorescence components. The DAS of apo CDOM33 is shown in Fig. 1. While the binding of Ca²⁺ to apo CDOM33 could clearly be detected by changes in the fluorescence parameters, interaction of Ca²⁺ with

peptide 33 was not evident from the fluorescence behavior, confirming the results of MacManus *et al.* [3]. Binding of Mg²⁺ and Tb³⁺ ions to both peptide 33 and CDOM33 was detectable by changes in the parameters relative to those of the apo protein. Quenching of the fluorescence signal by Tb³⁺ was considerably greater in CDOM33 than in peptide 33, confirming previous steady-state fluorescence studies [3,4]. In all forms of CDOM33, however, there was no significant change in the steady-state fluorescence emission maximum (345 nm). In contrast to CDOM33, it can be seen that 5HW-CDOM33 fluorescence parameters were relatively insensitive to metal addition, with Ca²⁺ binding producing negligible change and Mg²⁺ binding being detected by only small changes in τ_2 and the relative concentration of components. Tb³⁺ quenches the fluorescence of 5HW in 5HW-CDOM33, but not to the same extent as Trp fluorescence quenching in CDOM33. Figure 2 shows the effect of Ca²⁺ titration on the Trp fluorescence intensity from CDOM33. It can be seen that the quantum yield increased upon Ca²⁺ binding (0.10 to 0.15), with stoichiometric binding occurring to the CD and EF sites. Binding of Mg²⁺ to CDOM33 was also observable by a quantum yield increase (Fig. 3), but the affinity was clearly lower than that of Ca²⁺.

When 5HW was incorporated into Y57W [9], the fluorescence parameters were again relatively insensitive to binding of metal ions (Table II). Tb³⁺ binding slightly quenched the fluorescence and also resulted in a triple-exponential fluorescence decay. Data from Hutnik *et al.* [5] are given for comparison and show that the Trp res-

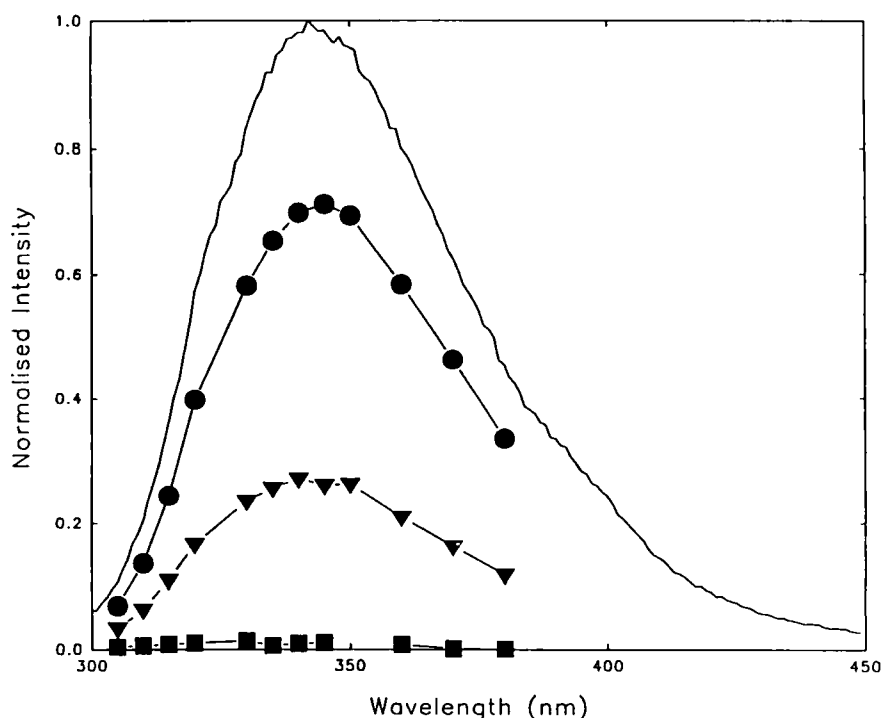


Fig. 1. Decay-associated spectra of apo CDM33. The corrected steady-state fluorescence spectrum of $5 \mu\text{M}$ apo CDM33 (solid line) was used to calculate the decay-associated spectra, by using the fractional intensities of each fluorescence lifetime component at 12 wavelengths: 5.81 ns, circles; 1.64 ns, triangles; 0.27 ns, squares.

idue in Y57W is clearly sensitive to Ca^{2+} binding to the apo protein.

DISCUSSION

The effects of the cassette replacement of the CD site in oncomodulin with a consensus sequence peptide were studied by comparison of the fluorescence parameters of the Trp incorporated at position 7 of the wild-type sequence (Y57W) and in the consensus sequence (CDM33). From Table I it can be seen that the consensus peptide had quite different fluorescence characteristics than when it was incorporated into the CD site of oncomodulin, suggesting different conformations of the sequence in the free and incorporated structures. Conformational freedom of the peptide is expected to be dramatically reduced when held between the C and the D helices of oncomodulin.

The changes in the fluorescence parameters in going from apo peptide 33 to apo CDM33 were significant, although the decays were both triple exponential, suggesting that the indole side chain was not rotationally restricted either in the protein or in the free peptide. The binding of Ca^{2+} ions to peptide 33 does not alter the

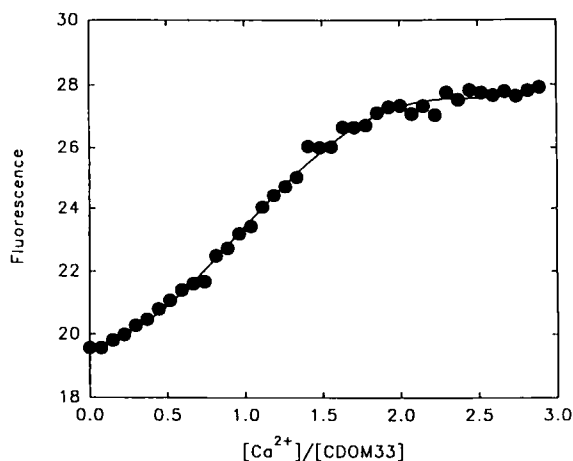


Fig. 2. Fluorescence titration of CDM33 with Ca^{2+} . Apo CDM33, $5 \mu\text{M}$ ($1960 \mu\text{l}$), was titrated with $40 \times 1.5\text{-}\mu\text{l}$ aliquots of Ca^{2+} ($500 \mu\text{M}$) to produce a final ratio of $\text{Ca}^{2+}/\text{CDM33}$ of 3:1. Excitation was at 290 nm and emission was at 350 nm.

environment of the Trp residue as the fluorescence lifetimes and quantum yields remained essentially unchanged. This is in contrast to Ca^{2+} binding to the same sequence in the CD loop of oncomodulin (CDM33). The environment of the Trp residue was affected, as re-

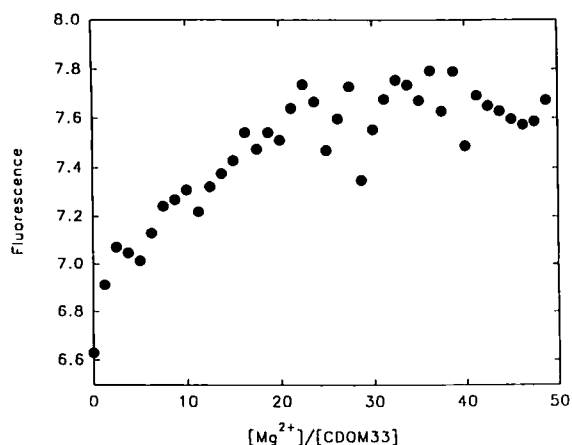


Fig. 3. Fluorescence titration of CDOM33 with Mg²⁺. Apo CDOM33, 5 μ M (2000 μ l), was titrated with 40 \times 2.5 μ l aliquots of Mg²⁺ (5 mM) to produce a final ratio of Mg²⁺/CDOM33 of 50:1. Excitation was at 290 nm and emission was at 350 nm.

flected in changes in fluorescence lifetimes and component concentrations and a quantum yield increase (Fig. 2). When the data from Y57W were compared with those from CDOM33, it appeared that the other residues in the loop had a significant effect on the environment and structure of the Trp residue, as seen by the very different decay time values for the apoproteins and differences in the relative concentration terms, especially for the Ca²⁺-loaded forms of the proteins (Tables I and II). Addition of Ca²⁺ to Y57W caused a decrease in Trp fluorescence quantum yield [5], as opposed to the quantum yield increase reported here for CDOM33. Clearly there are structural differences in the loop and Trp conformation upon replacement of the wild-type sequence with the consensus sequence in the CD loop, as well as differences in the Ca²⁺-binding affinities of the two forms of the CD loop. The D59E mutant of oncomodulin was previously shown to have a slightly increased Ca²⁺ affinity in the CD loop compared to the wild-type protein [6]. In the Y57W mutant of the protein, the maximum Trp fluorescence response occurred after the addition of one molar equivalent of Ca²⁺, yet the EF loop was filling first. Hence the titration in Fig. 2 suggested that the CD loop in CDOM33 has an affinity comparable to that of the EF loop. This is in contrast to the wild-type CD loop, which has a 10-fold lower Ca²⁺ affinity than the EF loop [6,7]. Taken together, these points suggest that the consensus CD loop in CDOM33 has an approximately 10-fold higher affinity for Ca²⁺ than the wild-type CD loop of oncomodulin.

When Mg²⁺ was added to both peptide 33 and CDOM33, a change in the Trp fluorescence parameters

was observed. It is surprising that Trp fluorescence from peptide 33 responded to Mg²⁺ addition but not Ca²⁺ addition. There was a clear Mg²⁺ effect in CDOM33 that was different from that of Ca²⁺ but, again, involved a quantum yield increase which was titratable (Fig 3). Coupled with the 10-fold higher Ca²⁺ affinity, the Mg²⁺ effect suggested that the cassette mutagenesis converted the Ca²⁺-specific CD site of oncomodulin into a Ca²⁺/Mg²⁺ site in CDOM33 [6,20,21]. This further suggests that the metal ion specificity of a HLH site is partially controlled by the residues in the individual loops, without a contribution from the tertiary structure of the rest of the protein.

The fluorescence lifetimes of Tb³⁺-loaded CDOM33 confirmed the very effective quenching of Trp fluorescence by Tb³⁺ observed earlier [4]. The relative concentration terms obtained from the DAS of the Tb³⁺ complexes with CDOM33, 5HW-CDOM33, and Y57(5HW) indicate that the Tb³⁺-loaded CD loops have very different structures from the Ca²⁺- or Mg²⁺-filled loops. If the different decay times can be assigned to different rotamer states of the Trp residue [24], then it would appear that in the Tb³⁺-loaded CDOM33, one conformation of the Trp residue dominated. Interestingly, the Trp residue in the Ca²⁺-filled loop in Y57W appears to have the same conformational distribution as it does in the Tb³⁺-loaded CDOM33. The Tb³⁺-loaded peptide 33 produced slightly quenched Trp fluorescence compared to the CDOM33 species [3,4], but the relative concentration terms were similar to those of the apo peptide. This indicated that the conformation of the peptide near the Trp residue in the Tb³⁺/peptide complex was similar to that in the apo peptide. This contrasts to the changes observed when Tb³⁺ bound to the protein. The affinity of the peptide for Tb³⁺ was lower than that of CDOM33, probably because of a more compact conformation of the Tb³⁺-loaded loop in the protein and lack of any flanking helices. A reduction in the Trp \rightarrow Tb³⁺ distance in the protein, as well as the exclusion of water from the Tb³⁺-filled loop, would result in significantly more efficient energy transfer.

Incorporation of 5HW into both Y57W and CDOM33 allowed examination of the ability of this new intrinsic probe [4,22] to report on conformational changes within proteins. While Y57(5HW) could be separated from Y57W leakage product [9], the separation of CDOM33 and 5HW-CDOM33 by comparable HPLC methods could not be achieved. However, fluorescence data from 5HW-CDOM33 were collected by selective excitation of 5HW at 310 nm. This ability to study the protein of interest in the presence of other Trp-containing species is one of the main advantages of novel, Trp

Table II. Time-Resolved Fluorescence Parameters of Tryptophan in Y57W Oncomodulin*

	τ_1 (ns)	τ_2 (ns)	τ_3 (ns)	C_1	C_2	C_3	χ^2	SVR
Y57(SHW)								
Apo	3.32	1.03		0.73	0.27		1.09	1.75
Ca ²⁺ loaded	3.34	1.08		0.73	0.27		1.07	1.79
Mg ²⁺ loaded	3.35	1.09		0.72	0.28		1.07	1.79
Tb ³⁺ loaded	3.13	1.09	0.14	0.25	0.39	0.36	1.09	1.74
Y57W ^b								
Apo	5.25	2.05	0.50	0.24	0.51	0.25		1.98
Ca ²⁺ loaded	6.17	1.61	0.37	0.09	0.75	0.17		1.98

* $C_1 + C_2 + C_3 = 1$, where $C_i = (\text{DAS, area}/\tau_i)$. DAS, decay-associated spectrum. Typical SE: $\tau_1 = \pm 0.01$ ns; $\tau_2 = \pm 0.02$ ns; $\tau_3 = \pm 0.002$ ns. Error in C_i no more than 5%.

^bFrom Ref. 5.

analogue intrinsic probes with red-shifted absorption spectra relative to that of Trp. The results summarized in Tables I and II suggest that SHW was relatively insensitive to changes in local structure. The significant fluorescence changes associated with Ca²⁺ binding to apo Y57W and CDOM33 were absent in Y57(SHW) and SHW-CDOM33. Apo and holo Y57(SHW) and SHW-CDOM33 all had essentially the same fluorescence parameters, with only Mg²⁺-loaded SHW-CDOM33 exhibiting a small change with respect to the apo protein. It is notable that only double-exponential decay kinetics were observed in these cases, with the exception of Tb³⁺-loaded Y57(SHW). Either the conformation of the SHW residue was restricted or two of the side-chain conformers have similar decay times. Quenching of the SHW fluorescence in both proteins by Tb³⁺ was analogous to that in Y57W and CDOM33 [4], with considerably more quenching found in the CDOM33 species. It is not clear whether this insensitivity is an intrinsic property of SHW or whether some other process, such as hydrogen bonding of the hydroxyl group, is preventing the residue from reporting subtle changes in its electronic environment. Interestingly, the oncomodulin mutant Y65F, which had a hydroxyl group at position 57 in the Tyr residue, exhibited three exponential decay components and was sensitive to Ca²⁺ binding, as measured through changes in Tyr fluorescence parameters [5].

The main conclusion from this work is that CDOM33 has CD loop properties quite different from those of Y57W, as determined from Trp fluorescence parameters. The consensus sequence has conferred Ca²⁺/Mg²⁺ specificity to the CD site which was Ca²⁺ specific in the wild-type protein. This demonstrated the importance of the residues in the binding loop for determining metal ion specificity. Also, the structures of the Tb³⁺-loaded forms were different from those of the other metal-saturated forms of these proteins. The ability of

the proteins to adapt to different structures on binding Tb³⁺ may alter their relative binding affinities or order of fill with Tb³⁺. In attempting to confirm these conclusions with a different chromophore, this study suggests that the novel intrinsic probe, SHW, is a poor reporter of conformational changes in these proteins. Further evidence of the insensitivity of SHW as an environment probe is found in the small changes observed in the fluorescence parameters of SHW before and after binding to the hydrophobic Trp-binding site in *B. subtilis* tryptophanyl-tRNA synthetase [23]. It has been shown previously, however, that SHW is a useful intrinsic probe for fluorescence anisotropy measurements for the study of protein/protein [9] and protein/DNA [22] interaction.

ACKNOWLEDGMENTS

The technical assistance of Mr. D. T. Krajcarski is gratefully acknowledged. C. M. V. Hogue is the holder of a National Science and Engineering Research Council (NSERC) Scholarship for graduate studies. This research was supported in part by a grant to A. G. Szabo from the NSERC. A. J. Bruckman is a NRC summer student (1993).

REFERENCES

1. N. C. J. Strynadka and M. N. G. James (1989) *Annu. Rev. Biochem.* **58**, 951–998.
2. B. J. Marsden, G. S. Shaw, and B. D. Sykes (1989) *Biochem. Cell Biol.* **68**, 587–601.
3. J. P. MacManus, C. W. Hogue, B. J. Marsden, M. Sikorska, and A. G. Szabo (1990) *J. Biol. Chem.* **265**, 10358–10366.
4. C. V. W. Hogue, J. P. MacManus, D. Banville, and A. G. Szabo (1992) *J. Biol. Chem.* **267**, 13340–13347.
5. C. M. L. Hutnik, J. P. MacManus, D. Banville, and A. G. Szabo (1991) *Biochemistry* **30**, 7652–7660.

6. R. C. Hapak, P. J. Lammers, W. A. Palmisano, E. R. Birnbaum, and M. T. Henzl (1989) *J. Biol. Chem.* **264**, 18751–18760.
7. J. A. Cox, M. Milos, and J. P. MacManus (1990) *J. Biol. Chem.* **265**, 6633–6637.
8. J. J. Falke, E. E. Snyder, K. C. Thatcher, and C. S. Voertler (1991) *Biochemistry* **30**, 8690–8697.
9. C. W. V. Hogue, I. Rasquinha, A. G. Szabo, and J. P. MacManus (1992) *FEBS Lett.* **310**, 269–272.
10. J. P. MacManus, C. M. L. Hutnik, B. D. Sykes, A. G. Szabo, T. C. Williams, and D. Banville (1989) *J. Biol. Chem.* **264**, 3470–3477.
11. C. M. Hutnik, J. P. MacManus, D. Banville, and A. G. Szabo (1990) *J. Biol. Chem.* **265**, 11456–11464.
12. K. J. Willis and A. G. Szabo (1989) *Biochemistry* **28**, 4902–4908.
13. K. J. Willis, A. G. Szabo, and D. T. Krajcarski (1990) *Photochem. Photobiol.* **51**, 375–377.
14. D. W. Marquardt (1963) *J. Soc. Ind. Appl. Math.* **11**, 431–441.
15. J. Durbin and G. S. Watson (1971) *Biometrika* **58**, 1–19.
16. M. Zuker, A. G. Szabo, L. Bramall, D. T. Krajcarski, and B. Selinger (1985) *Rev. Sci. Instrum.* **56**, 14–22.
17. J. R. Knutson, J. M. Beechem, and L. Brand (1983) *Chem. Phys. Lett.* **102**, 501–507.
18. J. R. Knutson, D. G. Walbridge, and L. Brand (1982) *Biochemistry* **21**, 4671–4679.
19. S. R. Meech and D. Phillips (1983) *J. Photochem.* **23**, 193–217.
20. M. Goodman, J.-F. Pechère, J. Haiech, and J. Demaille (1979) *J. Mol. Evol.* **13**, 331–352.
21. J. Haiech, J. Derancourt, J.-F. Pechère, and J. G. Demaille (1981) *Biochemistry* **20**, 3890–3897.
22. J. B. A. Ross, D. F. Senear, E. Waxman, B. B. Kombo, E. Rusinova, Y. T. Huang, W. R. Laws, and C. A. Hasselbacher (1992) *Proc. Natl. Acad. Sci. USA* **89**, 12023–12027.
23. C. W. V. Hogue and A. G. Szabo (1993) *Biophys. Chem.* **48**, 158–169.
24. A. G. Szabo and D. M. Rayner (1980) *J. Am. Chem. Soc.* **102**, 554–563.